Available online at www.sciencedirect.com
ScienceDirect
Intermetallics 16 (2008) 262–266
Intermetallics
www.elsevier.com/locate/intermet

Thermodynamic calculation and experimental investigation of glass formation in Zr–Ni–Ti alloy system

X.J. Liu, X.D. Hui*, G.L. Chen

State Key Laboratory for Advanced Metals and Materials, University of Science and Technology Beijing, 30 Xueyuan Road, Haidian District, Beijing 100083, China

Received 26 June 2007; received in revised form 8 October 2007; accepted 10 October 2007
Available online 20 December 2007

Abstract

Based on the undercooling theory resulting from the existence of multicomponent chemical short-range order domains, the glass forming range (GFR) in Zr–Ni–Ti alloy system was predicted by thermodynamic calculation. In order to verify the calculated results, a series of alloys $Zr_{90-x}Ni_xTi_{10}$ ($x = 25$, 30, 35, 40, 45, 50, 55 at.%) were designed to conduct melt-spinning experiments. The X-ray diffraction (XRD) results show that a fully amorphous structure can be obtained in as-quenched $Zr_{90-x}Ni_xTi_{10}$ ($x = 25$, 30, 35, 40, 45 at.%) alloys, while $Zr_{40}Ni_{50}Ti_{10}$ and $Zr_{35}Ni_{55}Ti_{10}$ alloys are partially amorphous and fully crystalline, respectively. These experimental results are consistent with the predicted GFR. In addition, the glass forming ability (GFA) was investigated by differential scanning calorimetry (DSC) experiments and evaluated by a thermodynamic parameter, the reduced undercooling ΔT_r.

Keywords: B. Glasses, metallic; C. Rapid solidification processing; E. Phase stability, prediction; F. Diffraction

1. Introduction

Metallic glasses, for their unique properties and different structures, in contrast to conventional crystals, have attracted many scientists' attention since the first success of preparing an amorphous phase in the Au–Si system by solidification in 1960 [1]. Last two decades, the discovery of the bulk metallic glass (BMG), with critical cooling rates as slow as 1–100 K/s, has triggered tremendous research activity in this area [2–8]. That is because: (1) bulk amorphous samples can be obtained via conventional metal processing such as Cu-mold casting and (2) the occurrence of BMGs promise new structural application. The understanding of glass forming criteria is a very important and open question for the design of new alloy systems. So far, the reduced glass transition temperature T_{rg} ($=T_g/T_l$, where T_g and T_l are glass transition temperature and liquidus temperature, respectively) [9] and γ [$=T_x/(T_g + T_l)$, where T_x is the onset of crystallization temperature] [10] are two of the most effective parameters used to evaluate the glass forming ability (GFA). Meanwhile, some empirical rules, such as the eutectic line rule [11], three empirical rules [7] and the rule of constant electron concentration and constant atomic size [12], have been proposed to act as a guideline in the design of new alloy composition. These rules have a key role in searching new alloy composition. However, their applicability is inevitably limited by the fact that most of them are ''rule of thumb'', and the traditional trial and error method is extensively used in exploring novel compositions as yet.

Recently, some efforts [13–17] have been conducted to estimate the glass forming ability (GFA) and predict the glass forming range (GFR) based on thermodynamic calculation. In particular, the thermodynamic calculation based on the calculation of phase diagrams' (CALPHAD) approach has been extensively used to estimate the GFA of alloys [15–17]. Thermodynamic properties such as enthalpies, activities, and phase equilibria are taken into account in the thermodynamic assessments; however, the short range ordering is usually missing and recognized as the most neglected quantities of all the

* Corresponding author. Tel.: +86 10 62333066; fax: +86 10 62333447.
E-mail address: xdhui@skl.ustb.edu.cn (X.D. Hui).

0966-9795/$ - see front matter © 2007 Elsevier Ltd. All rights reserved.
doi:10.1016/j.intermet.2007.10.007

thermodynamic properties, with respect to experimental investigations. In other words, no short range ordering and random mixing are assumed in the liquid [16]. This is a good assumption for the case where interactions between constituents in the liquid phase are small. However, for compound-forming systems, characterized by large negative interaction energies between constituents, just as many bulk glass forming systems, this assumption is not valid. In fact, chemical short-range order (CSRO) with different compound-types and icosahedral topological short-range order (TSRO) were observed by using high resolution transmission microscope (HRTEM) coupled with nano-beam diffraction technique in previous work [18,19]. Based on these experimental results, an undercooling theory resulting from the existence of multicomponent chemical short-range order (MCSRO) domain in multicomponent metallic melts has been proposed. Moreover, a thermodynamic model based on the undercooling theory of MCSRO has been constructed and successfully applied in prediction of GFR in Zr–Cu–Ni alloy system. In this paper, the aim is to predict the GFR and evaluate the GFA in Zr–Ni–Ti ternary system by thermodynamic calculation and experimental investigation. The reason why Zr–Ni–Ti alloy system was selected is that: first, most works [20–22] on Zr–Ni–Ti ternary alloy were dealt with quasicrystals, but few researches were focused on the amorphous. Second, the Zr–Ni–Ti ternary alloy system can be taken as the primary alloy of many Zr-based BMG alloy systems.

2. Thermodynamic calculation

Amorphous structures are often treated as a homogeneous liquid-like structure. Recently, however, many works [19,23] indicated that there is always a strong tendency to form intermetallic compounds in the glassy forming metallic melts, resulting in composition fluctuation in the melts. One of the representative cases implying the non-uniform feature of amorphous structure is the phase separation, which is often observed in the metallic glasses [24]. A reasonable explanation of this phenomenon is argued that there exist multicomponent chemical short-range orders (MCSRO) in a multicomponent glass forming metallic melt. Actually, different CSROs with face-centered cubic (FCC) Zr_2Ni-type and body-centered tetragonal (BCT) Zr_2Ni-type have been observed in the Zr-based bulk metallic glasses [18,19]. Based on this observation, an undercooling theory, resulting from the existence of MCSRO domain in multicomponent metallic melts, has been proposed, which means that a larger undercooling is required for solidification of the metallic melts with MCSRO comparing with that in ideal metallic melts. The undercooling of MCSRO $\Delta T_{\mathrm{MCSRO}}$ is defined as the difference between the values in the metallic melts with MCSRO and that in the ideal metallic melts [13,19], i.e.,

$$\Delta T_{\mathrm{MCSRO}} = \frac{(H_{\mathrm{L}} - H_{\mathrm{MCSRO}}) - T_{\mathrm{MCSRO}}(S_{\mathrm{L}} - S_{\mathrm{MCSRO}})}{L_{\mathrm{m}}} T_{\mathrm{m}} = (G_{\mathrm{homo}} - G_{\mathrm{MCSRO}})/\Delta S_{\mathrm{m}} = \Delta G_{\mathrm{MCSRO}}/\Delta S_{\mathrm{m}} \quad (1)$$

where T_{m} and L_{m} are melting temperature and enthalpy of melting, respectively. G_{homo}, G_{MCSRO} and ΔS_{m} are Gibbs free energy for ideal melts (homo-melts) and real melts including MCSRO and entropy of fusion, respectively. The Eq. (1) shows that the undercooling of MCSRO $\Delta T_{\mathrm{MCSRO}}$ is proportional to $\Delta G_{\mathrm{MCSRO}}$, the difference of Gibbs free energy between G_{homo} and G_{MCSRO}, but is the reciprocal of ΔS_{m}. Moreover, it is believed that the higher is the $\Delta T_{\mathrm{MCSRO}}$ the better is the GFA in an alloy system. Thus, one can evaluate the GFA and predict the GFR by calculating the $\Delta T_{\mathrm{MCSRO}}$ in an alloy system. In this case, we only calculated the $\Delta G_{\mathrm{MCSRO}}$. According to previous works [19,25], the G_{MCSRO} can be obtained by following formula:

$$\begin{aligned} G_{\mathrm{MCSRO}} = {} & \sum_{i=1}^{N-1}\sum_{j=i+1}^{N}\sum_{k=1}^{M}\left(n_{A_i^{k1}A_j^{k2}}\Delta G^0_{A_i^{k1}A_j^{k2}}\right) + \sum_{i=1}^{N-2}\sum_{j=1+1}^{N-1}\sum_{l=i+2}^{N} \\ & \times \sum_{p=1}^{Q} n_{A_i^{p1}A_j^{p2}A_l^{p3}}\Delta G^0_{A_i^{p1}A_j^{p2}A_l^{p3}} + RT\left[\sum_{i=1}^{N} n_i^0 \ln\left(n_i^0\gamma_i^0/n\right)\right. \\ & \left. + \sum_{i=1}^{N-1}\sum_{j=i+1}^{N}\sum_{k=1}^{M} n_{A_i^{k1}A_j^{k2}} \ln\left(n_{A_i^{k1}A_j^{k2}}\gamma_{A_i^{k1}A_j^{k2}}/n\right)\right] + RT\sum_{i=1}^{N-2} \\ & \times \sum_{j=1+1}^{N-1}\sum_{l=i+2}^{N}\sum_{p=1}^{Q} n_{A_i^{p1}A_j^{p2}A_l^{p3}} \ln\left(n_{A_i^{p1}A_j^{p2}A_l^{p3}}\gamma_{A_i^{p1}A_j^{p2}A_l^{p3}}/n\right) \end{aligned} \quad (2)$$

where $\Delta G^0_{A_i^{k1}A_j^{k2}} = \mu^0_{A_i^{k1}A_j^{k2}} - k_1\mu^0_{A_i^0} - k_2\mu^0_{A_j^0}$. For the detailed definition of parameters used in Eq. (2) see Refs [19,25].

The thermodynamic model and numerical method used in this case are same as that described in the literatures [13,18,19,25], so the detail is not addressed here. It should be pointed out that the contribution of icosahedral short-range order (ISRO) was also taken into account in addition to MCSROs, due to the fact that a stable icosahedral quasicrystalline phase (I-phase) was found in Zr–Ni–Ti alloy system [20]. In the present case, however, the thermodynamic data about I-phase were instead of its 1/1-approximant (*W*-TiZrNi) [26] because we cannot get the thermodynamic data of I-phase in Zr–Ni–Ti alloy system. All thermodynamic data used in this calculation can be found in the literatures [26–29]. The thermodynamic calculation was implemented by our own Fortran code.

Fig. 1 shows the $\Delta G_{\mathrm{MCSRO}}$ dependence of composition in Zr–Ni–Ti undercooled melts. It can be seen that there are two maximums of $\Delta G_{\mathrm{MCSRO}}$ in the whole composition map. One composition zone (named as A zone) is $Zr_xNi_yTi_z$ ($45 \le x \le 70$, $27 \le y \le 47$, $0 \le z \le 15$ at.%) the other (named as B zone) is $Zr_xNi_yTi_z$ ($30 \le x \le 54$, $12 \le y \le 24$, $25 \le z \le 51$ at.%). By investigating the relationship between content of different SROs and the composition, it is found that the predominant SROs are various compound-types in A zone but *W*-TiZrNi in B zone. It is known that a crystal formation results from the phase competition or selection of all existing phases in the metallic melts. In the present case, the

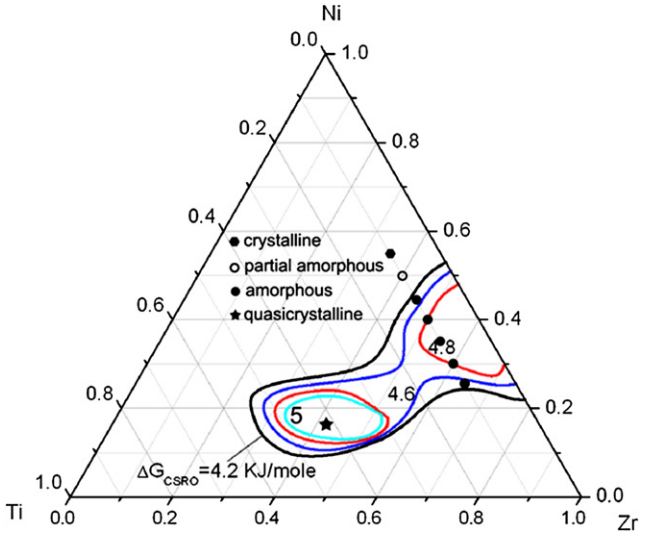

Fig. 1. Contour line (color online) of ΔG_{MCSRO} the difference in Gibbs free energy in Zr–Ni–Ti undercooled melts at 1273 K. A zone and B zone are the glass forming zone and quasicrystals forming zone, respectively. The stable I-phase $Zr_{41.5}Ni_{17}Ti_{41.5}$ [20] was marked as pentacle. The designed alloys were marked as dots and hexagon.

various SROs can act as nuclei or offer the sites for nucleation of their corresponding compounds. The presence of many SROs with different compound-types will enhance the complexity of phase competition, and then decrease the possibility of crystallization. On the other hand, however, the counterpart of SRO is easy to form if there is only one kind of SRO in the metallic melts. It is therefore argued that the GFR locates in A zone while I-phases form in B zone. In fact, the formation of I-phase in B zone has been confirmed by the discovery of a stable I-phase $Zr_{41.5}Ni_{17}Ti_{41.5}$, indicating that our calculation is effective. So, in the next section, the alloys' compositions located in A zone was selected to conduct experimental study.

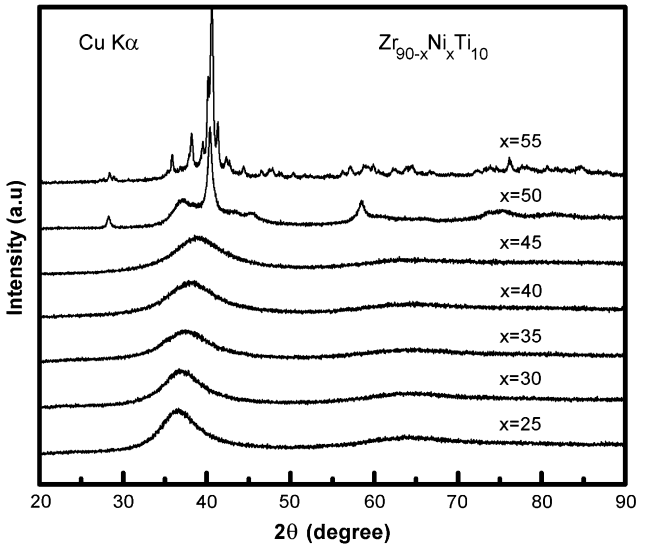

Fig. 2. XRD patterns of as-quenched $Zr_{90-x}Ni_xTi_{10}$ ($x = 25, 30, 35, 40, 45, 50, 55$ at.%) alloys.

3. Experimental procedure

Based on the results of thermodynamic calculation, a serials of compositions $Zr_{90-x}Ni_xTi_{10}$ ($x = 25$, 30, 35, 40, 45, 50, 55 at.%, as shown in Fig. 1) were designed to investigate. The master alloys were prepared by arc melting mixture of pure metals (≥99.9 wt.%) under a Ti-gettered pure argon atmosphere. The alloy ingots were remelted four times to ensure homogeneity. The ribbons with about 0.05 mm thickness and 5 mm broadness were produced by the vacuum single roller melt-spinning technique (the diameter of copper roller and line velocity are 200 mm and 30–35 m/s, respectively). X-ray diffraction (Cu Kα Philips APD-10) and transmission electron microscope (TEM, JEOL 2000FX, operating at 160 kV) were exploited to check the structural nature of samples. The differential scanning calorimetry (DSC) experiments to determine some related characteristic temperatures of samples were performed at Netzsch 449C. The thin foil for TEM analysis was prepared electrolytically by twinjet polishing under 240 K in a mixture of 90 vol% methanol and 10 vol% perchloric acid.

4. Results and discussion

4.1. Glass forming range (GFR)

Fig. 2 shows the X-ray diffraction (XRD) patterns of as-quenched $Zr_{90-x}Ni_xTi_{10}$ ($x = 25, 30, 35, 40, 45, 50, 55$ at.%) ribbons. It can be seen that there are no detectable crystalline peaks except for diffused halos when x increases from 25 to 45, indicating that these alloys are of fully amorphous structure. The fully amorphous nature was also confirmed by the transmission electron microscopy (TEM) observations (Fig. 3). While x increases to 50, some acute crystalline peaks were imposed on the amorphous halo, implying that the structure of this alloy is a composite state comprised of amorphous and crystalline phases. When x further increases to 55, the structure of as-quenched alloy

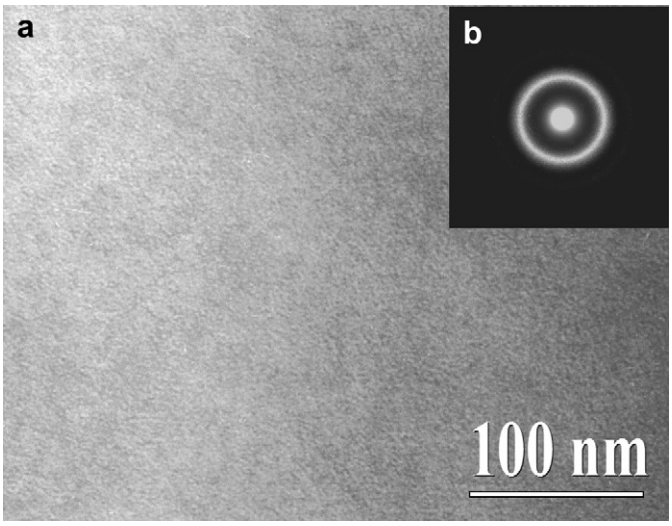

Fig. 3. TEM bright image (a) and corresponding SAD pattern (b) of as-quenched $Zr_{65}Ni_{25}Ti_{10}$ metallic glasses.

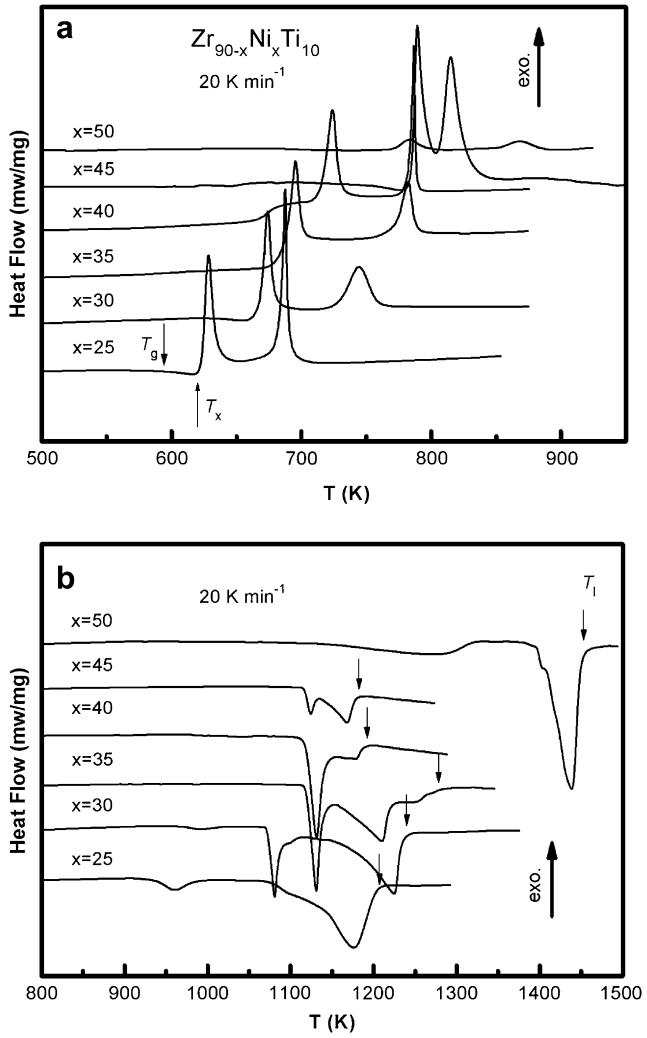

Fig. 4. DSC curves (a) and melting traces (b) of as-quenched $Zr_{90-x}Ni_xTi_{10}$ ($x = 25$, 30, 35, 40, 45, 50 at.%) alloys.

is almost consisted of crystalline phases due to the fact that only acute diffraction peaks can be found in its XRD pattern (Fig. 2). According to Fig. 1, one can found that those fully amorphous alloys with compositions of $Zr_{90-x}Ni_xTi_{10}$ ($x = 25$, 30, 35, 40, 45 at.%) are all located in the glass forming region (A region in Fig. 1) obtained by thermodynamic calculation, which confirmed the validity of our thermodynamic calculation.

An amorphous structure is essentially formed by suppressing the nucleation and growth of nuclei during the cooling of metallic melts, thus it is controlled by not only thermodynamic factor also kinetic one. Thermodynamically, the existence of MCSROs will increase the critical work to nucleation, because the competitive growth of a variety of SROs upon melt cooling, leading to formation of one type of nucleus needs to decompose those different structural SROs, and thus an additional energy is required. Therefore, a larger critical undercooling is required for nucleation in the melts with MCSROs. Kinetically, the nucleation and growth of nuclei is mainly implemented by diffusion of atoms. The existence of MCSROs in glass forming metallic melts will lead to: (i) increase in the distance of path of atomic diffusion due to the presence of different SROs; (ii) depress in the mobility of atoms and make the atomic diffusion very difficult owing to the drastic increase of viscosity of melts resulting from the increase of critical undercooling (i.e., descending temperature). As mentioned above, it is known that the existence of MCSROs in alloy melts is favored to form amorphous state in contrast to depress in nucleation and growth of nuclei. Now, it is not difficult to understand the reason why the GFR region determined by thermodynamic calculation can coincides very well with the experimental results, i.e., there are much more types and higher concentration of MCSROs in this GFR region.

4.2. Glass forming ability (GFA)

Fig. 4 shows the differential scanning calorimetry (DSC) curves (Fig. 4a) and melting traces (Fig. 4b) of designed alloys. In Fig. 4a, it can be seen that the crystallization of all these alloys is proceeded through a double-stage mode and the glass transition temperature T_g and onset temperature of crystallization T_x increased with increasing Ni content from 25% to 45%. While when Ni content reaches up to 50%, the enthalpy of crystallization becomes significantly less comparing with those in the alloys with Ni content from 25% to 45%, implying that there is only a small account of amorphous phase in this alloy. This is a good agreement with the XRD results. The liquidus temperature T_l and other thermodynamically characteristic temperatures obtained from Fig. 4 are all listed in Table 1. In order to evaluate the compositions' dependence of glass forming ability (GFA), reduced glass transition temperature T_{rg} ($=T_g/T_l$) and γ [$=T_x/(T_g + T_l)$] were calculated. The results show the values of T_{rg}, γ, T_g and T_x increased with the content of Ni increasing from

Table 1
Thermodynamic data of $Zr_{90-x}Ni_xTi_{10}$ ($x = 25$, 30, 35, 40, 45, 50 at.%), including T_g glass transition temperature, T_x onset temperature of crystallization, T_{p1} peak temperature of the first crystallization event, T_{p2} peak temperature of the second crystallization event, T_l liquidus temperature, ΔH_x enthalpy of crystallization, L_m enthalpy of melting, T_{rg} ($=T_g/T_l$) and γ [$=T_x/(T_g + T_l)$]

x	T_g	T_x	T_{p1}	T_{p2}	T_l	ΔH_x	L_m	T_{rg}	γ
25	593.0	623.2	628.9	687.4	1202.7	4.6	9.7	0.493	0.347
30	637.3	667.5	674.0	744.2	1232.8	4.7	10.0	0.517	0.357
35	656.2	687.9	695.5	782.1	1217.5	4.8	10.9	0.539	0.367
40	676.1	712.2	723.7	786.5	1203.9	4.5	4.8	0.562	0.379
45	759.7	786.1	788.9	814.9	1176.6	3.5	2.2	0.646	0.406
50	–	776.1	782.4	868.3	1448.1	3.3	8.8	–	–

The units of temperature and enthalpy are K and kJ/mol, respectively.

25% to 45%. In detail, when Ni content increases from 25% to 45%, T_{rg} and γ increased from 0.493 to 0.646 and from 0.347 to 0.406, respectively, as shown in Fig. 5. It is believed that the higher the value of T_{rg} or γ the better the GFA in an alloy system. Therefore, the best glass former is the alloy with a composition of $Zr_{45}Ni_{45}Ti_{10}$ in the case of Zr–Ni–Ti ternary system. It is expected that a bulk metallic glass (BMG) can be obtained by rationally introducing some alloyed elements into the alloy $Zr_{45}Ni_{45}Ti_{10}$. Actually, Xu et al. [30] have confirmed that a fully glassy sheet with a thickness of 0.5 mm can be formed in alloy $Zr_{35}Ni_{45}Ti_{20}$ and the critical thickness can be up to 5 mm by the addition of Al and Cu into the matrix alloy. If the Zr–Ni–Ti ternary system is treated as a Zr(Ti)–Ni pseudo-binary system, the best glass former $Zr_{45}Ni_{45}Ti_{10}$ in our case is then well agreed with the Xu's [30] experimental composition $Zr_{35}Ni_{45}Ti_{20}$.

It should be noted that the composition corresponding to the maximum of the ΔG_{MCSRO} in glass forming region (A zone in Fig. 1) is not $Zr_{45}Ni_{45}Ti_{10}$ but $Zr_{55}Ni_{35}Ti_{10}$ alloy. Meanwhile, it is known from Eq. (1) that the ΔT_{MCSRO} (GFA) is defined by the combination of ΔG_{MCSRO} and ΔS_m. Moreover, from Eq. (1) a reduced undercooling ΔT_r caused by MCSROs can be defined as follow:

$$\Delta T_r = \Delta T_{MCSRO}/T_m = \Delta G_{MCSRO}/L_m \quad (3)$$

where L_m is enthalpy of melting. GFA is proportional to ΔT_{MCSRO} and reciprocal to T_m, therefore, GFA is proportional to ΔT_r. The enthalpy of melting of alloys determined from Fig. 3b shows that alloy $Zr_{45}Ni_{45}Ti_{10}$ has a minimum of 2.2 kJ/mol, which is not more than half of the second small value (4.8 kJ/mol) among all the alloys. Taking the difference of ΔG_{MCSRO} among all the designed alloys into account (Fig. 1), it is safe to say that the ΔT_r for $Zr_{45}Ni_{45}Ti_{10}$ alloy is the largest one, i.e., the GFA of $Zr_{45}Ni_{45}Ti_{10}$ is predicted by thermodynamic calculation to be the best among all the designed alloys. This result implies that calculated results could be well consistent with experimental results if we take both ΔG_{MCSRO} and L_m into account in the thermodynamic calculation. The work only calculated that the ΔG_{MCSRO} is not enough to evaluate the GFA and the further work is under investigation.

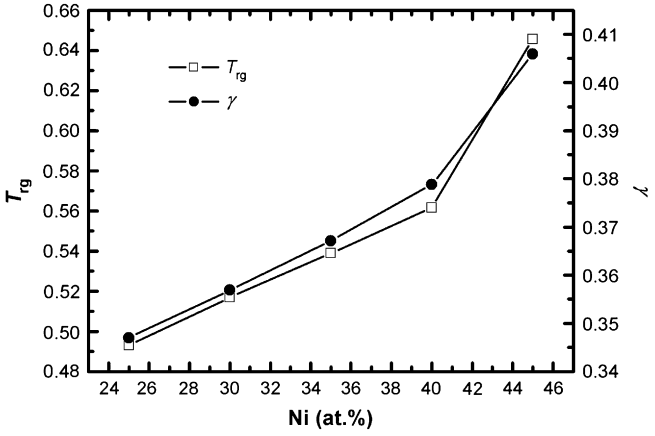

Fig. 5. Concentration dependence of the reduced transition temperature T_{rg} and γ in $Zr_{90-x}Ni_xTi_{10}$ ($x = 25, 30, 35, 40, 45$ at.%) metallic glasses.

5. Conclusion

(1) The GFR predicted by the thermodynamic calculation is consistent with the experimental results, the former is $Zr_xNi_yTi_z$ ($45 \le x \le 70, 27 \le y \le 47, 0 \le z \le 15$ at.%), and the latter is $Zr_{90-x}Ni_xTi_{10}$ ($x = 25, 30, 35, 40, 45$ at.%). This indicates that our thermodynamic calculation is reliable and offers an effective mean to design novel amorphous alloys.

(2) The experimental parameters T_{rg} and γ and thermodynamic parameter ΔT_r simultaneously show that the best glass former among all designed alloys is $Zr_{45}Ni_{45}Ti_{10}$.

(3) Not only ΔG_{MCSRO}, the difference of Gibbs free energy between G_{homo} and G_{MCSRO}, but also L_m, the enthalpy of melting, should be taken into account in the thermodynamic calculation.

Acknowledgments

This work was supported partly by the National Natural Science Foundation of China (Grant Nos. 50431030, 50471097,) and National Basic Research Program of China (2007CB613901).

References

[1] Klement W, Willens RH, Duwez P. Nature 1960;187(4740):869–70.
[2] Kui HW, Greer AL, Turnbull D. Appl Phys Lett 1984;45(6):615–6.
[3] Inoue A, Zhang T, Masumoto T. Mater Trans JIM 1990;31(3):177–83.
[4] Peker A, Johnson WL. Appl Phys Lett 1993;63(17):2342–4.
[5] Greer AL. Science 1995;267(3):1947–53.
[6] Johnson WL. Mater Res Bull 1999;24(10):42–56.
[7] Inoue A. Acta Mater 2000;48(1):279–306.
[8] Wang WH, Dong C, Shek CH. Mater Sci Eng 2004;R44:45–89.
[9] Turnbull D. Contemp Phys 1969;10(5):473–88.
[10] Lu ZP, Liu CT. Acta Mater 2002;50(13):3501–12.
[11] Davies HA, Lewis BG. Scr Met 1975;9(10):1107–12.
[12] Chen WR, Wang YM, Qiang JB, Dong C. Acta Mater 2003;51(7):1899–907.
[13] Hui XD, Chen GL, Ni XD, Bian Z. Trans Nonferrous Met Sco China 2001;11(5):684–91.
[14] Xia L, Fang SS, Wang Q, Dong YD, Liu CT. Appl Phys Lett 2006;88:171905.
[15] Shao G. Intermetallics 2003;11:313–24;
Shao G, Lu B, Liu YQ, Tsakiropoulos P. Intermetallics 2005;13:409–14.
[16] Abe T, Shimono M, Ode M, Onodera H. Acta Mater 2006;54:909–15.
[17] Ma D, Cao H, Chang YA. Intermetallics 2007;15:1122–6.
[18] Chen GL, Hui XD, He G, Bian Z. Mater Trans JIM 2001;42(6):1095–102.
[19] Chen GL, Hui XD, Fan SW, Kou HC, Yao KF. Intermetallics 2002;10(11-12):1221–32.
[20] Kelton KF, Kim WJ, Stroud RM. Appl Phys Lett 1997;70(24):3230–2.
[21] Yi S, Kim DH. J Mater Res 2000;15:892–7.
[22] Shaz MA, Mukhopadhyay NK, Mandal BK, Srivastava ON. J Alloys Compd 2002;342:49–52.
[23] Mattern N, Kühn U, Hermann H, Ehrenberg H, Neuefeind J, Eckert J. Acta Mater 2002;50(2):305–14.
[24] Busch R, Schneider S, Peker A, Johnson WL. Appl Phys Lett 1995;67(11):1544–6.
[25] Hui XD, Yao KF, Kou HC, Chen GL. Sci China 2003;E46(6):581–92.
[26] Kim WJ, Gibbons PC, Kelton KF, Yelon WB. Phys Rev B 1998;58:2578–85.
[27] Witusiewicz V, Sommer F. Metall Mater Trans 2000;B31(4):277–84.
[28] Thiedemann U, Rösner-Kuhn M, Drewes K, Kuppermann G, Frohberg MG. J Non-Cryst Solids 1999;250–252(1):329–35.
[29] Murray JL. The Ti–Zr system. Bull Alloy Phase Diag 1981;2(2):197–200.
[30] Xu DH, Duan G, Johnson WL, Garland C. Acta Mater 2004;52(12):3493–7.